ADVANCED FUNCTIONAL MATERIALS
www.afm-journal.de

Role of Side-Chain Branching on Thin-Film Structure and Electronic Properties of Polythiophenes

Scott Himmelberger, Duc T. Duong, John E. Northrup, Jonathan Rivnay, Felix P. V. Koch, Bryan S. Beckingham, Natalie Stingelin, Rachel A. Segalman, Stefan C. B. Mannsfeld, and Alberto Salleo**

Side-chain engineering is increasingly being utilized as a technique to impact the structural order and enhance the electronic properties of semiconducting polymers. However, the correlations drawn between structural changes and the resulting charge transport properties are typically indirect and qualitative in nature. In the present work, a combination of grazing incidence X-ray diffraction and crystallographic refinement calculations is used to determine the precise molecular packing structure of two thiophene-based semiconducting polymers to study the impact of side-chain modifications. The optimized structures provide high-quality fits to the experimental data and demonstrate that in addition to a large difference in interchain spacing between the two materials, there exists a significant disparity in backbone orientation as well. The calculated structures are utilized in density functional theory calculations to determine the band structure of the two materials and are shown to exhibit a dramatic disparity in interchain dispersion which accounts for the large observed difference in charge carrier mobility. The techniques presented here are meant to be general and are therefore applicable to many other highly diffracting semicrystalline polymers.

1. Introduction

Semiconducting polymers are of significant interest due to their potential low cost, mechanical flexibility, and compatibility with solution deposition techniques. The structure of these materials continues to be a topic of intense investigation due to the sensitivity of electronic properties to changes in the materials' microstructure. Relatively small changes to the chemical structure of a polymer, as well as variations in the processing conditions, can have rather dramatic effects on the molecular packing. Such detailed structural measurements have proven to be difficult however, in large part due to the inherent disorder in polymer systems, making the growth of extended single crystals extremely challenging. Thus, the continued development of techniques which will allow for the precise measurement of polymer microstructure remains one of the most important areas in this field of study.

In most semiconducting polymers, the inclusion of alkyl-based side chains is necessary in order to provide adequate solubility for compatibility with conventional solution deposition techniques. In recent years, side-chain engineering has begun to play an increased role not only in enhancing polymer processability, but in improving charge transport properties through structural modifications as well.[1–4] Tailoring of solubilizing groups to tune crystal structure has been utilized extensively in small molecules.[5–7] These systems form very crystalline structures where the solubilizing groups are relatively short and ordered and thus it can be

S. Himmelberger, D. T. Duong, Dr. J. Rivnay,[+] Prof. A. Salleo
Materials Science and Engineering
Stanford University
Stanford, CA 94305, USA
E-mail: asalleo@stanford.edu
Dr. J. E. Northrup
Palo Alto Research Center
Palo Alto, CA 94304, USA
Dr. F. P. V. Koch
Department of Materials
Eidgenössische Technische Hochschule (ETH)
Zürich 8093, Zurich, Switzerland
Dr. B. S. Beckingham, Prof. R. A. Segalman[++]
Materials Science Division
Lawrence Berkeley National Laboratory
Berkeley, CA 94720, USA

DOI: 10.1002/adfm.201500101

Prof. N. Stingelin
Centre for Plastic Electronics
Imperial College London
London SW7 2AZ, UK
Prof. R. A. Segalman
Department of Chemical and Biomolecular Engineering
University of California
Berkeley, CA 94720, USA
Prof. S. C. B. Mannsfeld
Center for Advancing Electronics Dresden
Dresden University of Technology
01062 Dresden, Germany
E-mail: stefan.mannsfeld@tu-dresden.de
[+]Present address: Department of Bioelectronics, Ecole Nationale Supérieure des Mines, CMP-EMSE, MOC, Gardanne, France
[++]Present address: Department of Chemical Engineering, University of California, Santa Barbara, CA 93106, USA

expected that modifying their structure will have a large effect on the resulting molecular packing. However, in polymer systems with disordered side chains, it is not readily apparent that the backbone crystalline structure will be impacted by modifications to the side chains. Improvements in polymer electronic properties have been correlated to variations in microstructure for a number of side-chain modification strategies; however, these observations have only focused on rather coarse measures of molecular packing and crystalline quality over large volumes of material.[8–10] Mei et al. demonstrated that by replacing the branched side chains of an isoindigo-based polymer with a novel siloxane-terminated solubilizing group, the π-stacking distance could be reduced, resulting in a factor of six increase in the charge carrier mobility.[11] Similarly, a record high hole mobility in excess of 10 $cm^2\ V^{-1}\ s^{-1}$ was achieved by Kang et al. in a diketopyrrolopyrrole (DPP)-based polymer through smart side-chain engineering. The π-stacking distance was reduced by moving the side-chain branching position further from the chain backbone.[1] In addition, Yiu et al. demonstrated that replacing branched side chains with linear ones in another DPP-based polymer reduced the steric hindrance between neighboring chains and increased the crystalline coherence length.[12] Clearly, side-chain engineering is increasingly being used as a powerful technique to improve the properties of semiconducting polymers.

Poly(3-hexylthiophene) (P3HT) is no different in this regard. It is known to have a higher charge carrier mobility than its branched side-chain analog, poly(3-(2′-ethyl)hexylthiophene) (P3EHT), but no detailed structural comparison of the two materials has been performed and the only explanation offered for the difference in transport properties is a slightly shorter π-stacking distance in P3HT.[13] It is important to realize however that π-stacking distance is used in these cases as a proxy for efficiency of electron transfer. This quantity however is not necessarily simply related to only π-stacking distance,[14] and as a result we seek to also measure differences in molecular orientation and conformation between the two materials in order to build a robust correlation to their electronic properties. Indeed, while knowledge of these general structural changes is clearly important for understanding the impact of side-chain modification, there are undoubtedly subtle modifications in chain conformation occurring at the molecular level that also greatly affect the resulting electronic properties. We aim to use the model systems studied herein to quantitatively explore the effect of side-chain modifications on structural and electronic properties and present a general method which can in principle be used to study the structure of any semicrystalline polymer.

Polythiophenes are some of the most studied organic semiconductors in history. In particular, P3HT has developed into a model system for the organic electronics community owing to its longevity in the field, and relatively high performance in solar cells and thin film transistors. As such, there have been numerous structural studies of P3HT using various substrates, device geometries, and processing conditions and the general packing structure of P3HT is well known.[15] On most substrates, including silicon oxide, P3HT chains preferentially lie "edge-on" with respect to the substrate, packing in a lamellar structure with the alkyl side chains standing perpendicular to the substrate and the thiophene rings of adjacent chains lying face-to-face with each other.

Beyond this basic understanding of the structure however, there have been relatively few detailed studies exploring the precise packing of P3HT. Efforts to define a unit cell have focused on using X-ray diffraction (XRD), selected-area electron diffraction (SAED), nuclear magnetic resonance (NMR), and density functional theory (DFT).[16–22] Most of these studies have concluded similar structures for P3HT, but orthorhombic, monoclinic, and triclinic unit cells have all been proposed. This may be due in part to the lack of uniformity in processing conditions used, owing to the unique needs of each characterization technique, as well as the inherent difficulty in defining a unit cell for a disordered, semicrystalline polymer. Even fewer efforts have been made to characterize the exact conformation of P3HT within a unit cell[17,23–26] despite the importance of the precise molecular packing structure on the optoelectronic properties of a semiconducting material.[27,28] Indeed, transfer integrals in P3HT have been shown to be sensitive to small changes in backbone orientation, intermolecular separation, as well as relative shifts between adjacent molecules.[29] Further, those structures which have been proposed are either the result of force field calculations or experiments performed on specially prepared samples which have been processed in a manner quite different from what is used to make devices.

In this work, a combination of grazing incidence X-ray diffraction (GIXD) and crystallographic refinement calculations are used to determine the precise molecular packing of both a 13-mer P3HT oligomer ($(3HT)_{13}$) and P3EHT (≈36 monomers in length) (**Figure 1**). These refined crystal structures are then utilized in the calculation of electronic band structures by DFT. Previously, we have used this combination of techniques to study the packing in a number of small molecule systems;[30–34] however, this is the first time this method has been used to determine the structure of a polymer-like system. In the case of $(3HT)_{13}$, the basic crystallographic building block is similar to that of its macromolecular counterparts, despite slight changes in unit cell dimensions, and does not require the entire oligomeric structure to adequately describe the structure.[35] The precise packing structure of P3EHT on the other hand has not been studied in detail. Our results indicate that, contrary to P3HT, the backbones of adjacent P3EHT chains are significantly tilted with respect to one another. This tilt, together with the larger spacing between adjacent chains, results in smaller intermolecular coupling in P3EHT and is likely responsible for the lower charge carrier mobilities measured for this material.

2. Results and Discussions

2.1. Molecular Packing in $(3HT)_{13}$

The crystallographic refinement technique described here relies on the accurate determination of both the location and intensity of scattered X-rays in reciprocal space (q-space). The experimental GIXD setup is depicted in Figure 1c. The incident X-ray beam strikes the sample at a grazing incidence angle α and is scattered onto the 2D image plate detector set a distance L away. Owing to the disordered nature of polymeric systems, high molecular weight P3HT yields diffuse and overlapping diffraction spots which complicate intensity quantification

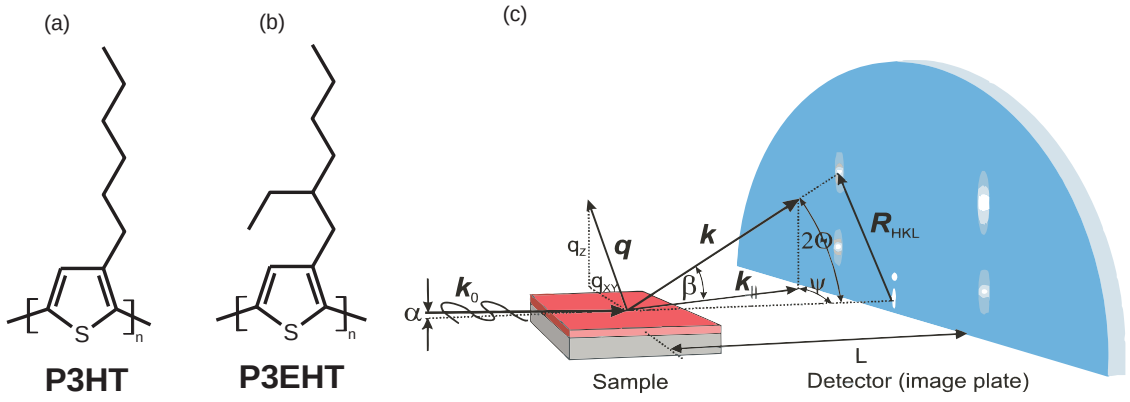

Figure 1. a) Chemical structure of P3HT. b) Chemical structure of P3EHT. c) Geometry of the GIXD setup. The incident beam k_0 forms an angle α with the sample surface; the intensity of the scattered beam k is recorded by an image plate detector at a distance L. The in-plane component of the momentum transfer vector, q, is q_{xy}; the vertical component is q_z. Reproduced with permission.[31] Copyright 2011, Wiley.

(Figure S1, Supporting Information). Recently, Koch et al. described the synthesis and general structural properties of a series of oligo(3-hexylthiophene)s ranging in length from 4 to 36.[36,37] They find, as we do here using the same set of materials, that P3HT changes from a polymorph with interdigitated side chains, Form II, to the more classical Form I beyond an oligomer length consisting of 12 repeat units. As such, we have chosen the shortest and perhaps most ordered oligo(3-hexylthiophene), $(3HT)_{13}$, which exhibits single phase, stable, and classic noninterdigitated packing of higher molecular weight P3HTs, for the refinement we describe here. The diffraction pattern recorded on the image plate for a thin film of $(3HT)_{13}$ is shown in **Figure 2**a. As can be seen in Figure S1, Supporting Information, the packing of $(3HT)_{13}$ is simply a more ordered representation of the structure of high molecular weight P3HT.

It must be specially noted that the diffraction images recorded directly by the image plate detector are distorted projections of q-space due to the flat nature of the detector and the curvature of the Ewald sphere. Before accurate peak positions could be determined, an image correction to account for this distortion must be applied. From the measurement of the accurate peak positions in the distortion-corrected image, the unit cell parameters could be determined, yielding a triclinic unit cell with $a = 7.72$ Å, $b = 5.46$ Å, $c = 15.62$ Å, $\alpha = 96.92°$, $\beta = 94.88°$, and $\gamma = 45.00°$. The triclinic unit cell contains two thiophene repeats along one $(3HT)_{13}$ chain and is in contrast to most published unit cells for P3HT which contain two chains and are described as orthorhombic. However, our unit cell is actually quite similar to those reported by others; we are able to reduce our unit cell to just one molecule after finding that adjacent chains are shifted by exactly one thiophene unit with respect to one another. The dimensions of the unit cell reported herein correspond to a density of 1.19 g cm^{-3}, slightly higher than the 1.12–1.14 g cm^{-3} which has been reported previously,[16,20,26,38] but this is likely due to the low disorder and highly crystalline nature of very low molecular weight P3HT used here.[35]

While the dimensions of the $(3HT)_{13}$ unit cell can be extracted solely from the diffraction peak positions, the precise atomic packing is contained in the structure factor of the molecule which manifests itself in the intensities of the diffraction peaks. Therefore, the molecular packing can be retrieved from the peak intensities by a refinement process. This is achieved by using a crystallographic refinement algorithm that fits theoretically calculated diffraction intensities to those measured by the area detector. The experimental peak intensity values were measured by integrating the diffraction peak intensities in boxes that tightly enclose the peak area after a line-wise linear background subtraction within these boxes. Theoretical expressions for the peak intensities were obtained from the structure factor square $|F_{hkl}|^2$ after several correction terms were applied to account for the specific GIXD scattering geometry and the properties of the synchrotron X-ray beam on SSRL BL 11-3 (details in refs. [16,31]. During the refinement process the molecular geometry and alignment of the molecule in the unit cell are varied, and for each configuration the crystallographic residual[39]—a type of least square error between theoretical and experimental intensity values—is calculated. This calculation is coupled to a Monte Carlo minimization algorithm that minimizes the crystallographic residual thereby determining the molecular unit cell configuration whose theoretical set of peak intensities is most similar to the set of measured peak intensities.

The refinement was initially performed on two simplistic, rigid-body models of $(3HT)_{13}$. The first was the model proposed by Kayunkid et al. ("tilted chain" model), determined from electron diffraction,[25] which contains alkyl side chains that are tilted relative to the thiophene backbone; the second model was constructed with the alkyl side chains coming straight off the conjugated backbone ("straight chain" model), parallel to the plane created by the thiophene rings. Both models yielded comparable but unsatisfactory fits to the experimental data. This is unsurprising given the different processing technique used to make the sample used in the "tilted chain" model, which likely generated a different structure than what we obtain by bar coating, and the unphysical nature of side chains which come off exactly parallel to the backbone plane in the "straight chain" model. Additionally, it is known from polarized IR transmission spectroscopy experiments that the alkyl side chains in P3HT contain some disorder.[40] While our model calculations require a crystalline unit cell (periodic boundary conditions), some flexibility was added

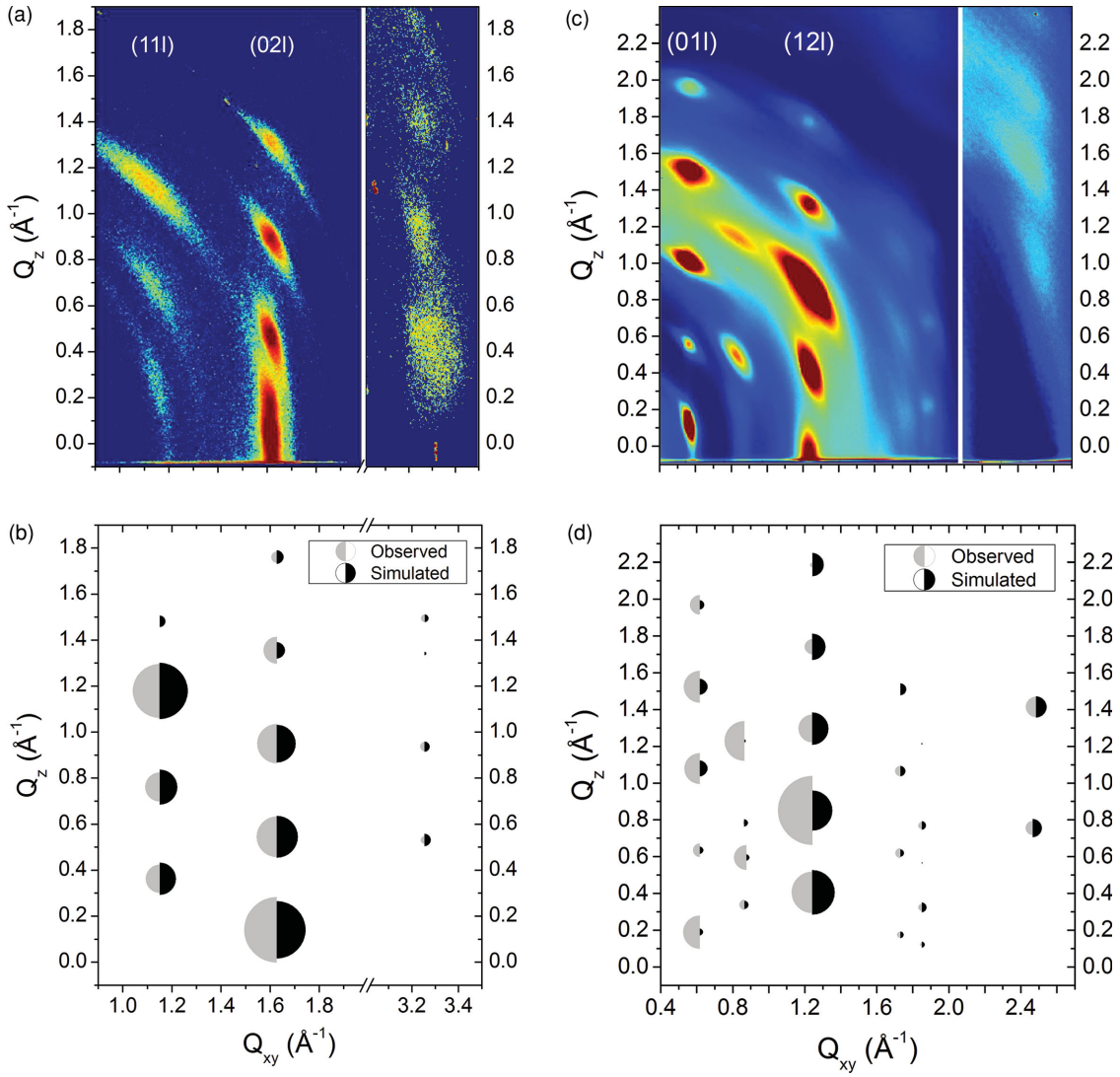

Figure 2. a) GIXD image of $(3HT)_{13}$ on SiO_2. b) Measured and calculated diffraction intensities (best-fit) for $(3HT)_{13}$ on SiO_2. c) GIXD image of P3EHT on SiO_2. d) Measured and calculated diffraction intensities (best-fit) for P3EHT on SiO_2. The diffraction intensity is indicated by the area of half-circles.

to our structure by inserting freely swinging "hinges" on the first and second carbon atoms of each alkyl side chain. These hinges allowed us to sample a multitude of different conformations including our original "straight chain" and "tilted chain" models without introducing an overwhelming number of degrees of freedom to the calculation. The result of the fit with hinges added is shown in Figure 2b. The size of each half-circle is representative of the measured and theoretical diffracted intensity at that point in *q*-space, respectively; we find that our model yields an excellent fit to the experiment as evidenced by the close match in the measured and calculated intensities over 13 peaks.

The best-fit structure after structural refinement is shown in **Figure 3**a,b. The simulated structure demonstrates that $(3HT)_{13}$ contains a tilted backbone which allows for greater electronic overlap between the delocalized π-orbitals on neighboring chains. While the repeat distance along the π-stacking direction corresponds to a spacing of ≈0.39 nm between adjacent thiophene rings, the backbone tilt creates a shorter perpendicular approach of the backbone planes of 0.36 nm. Additionally, we find a significant tilt in the alkyl side chains relative to the chain backbone. This allows the polymer lamellae to approach close to each other without interdigitation of the side chains. This structure is in agreement with measurements which indicate that the side chains of P3HT are spaced too closely to interdigitate.[40]

A schematic of the calculated structure labeled with key angles is given in Figure 3c,d,e while the corresponding angles are listed in **Table 1**. For comparison, two other detailed structural studies of P3HT conducted using different techniques are also included in the table.[25,26] Despite not providing an adequate fit to our experimental data, our structure bears considerable similarity to the structure proposed by Kayunkid et al.,[25] who used SAED to study low

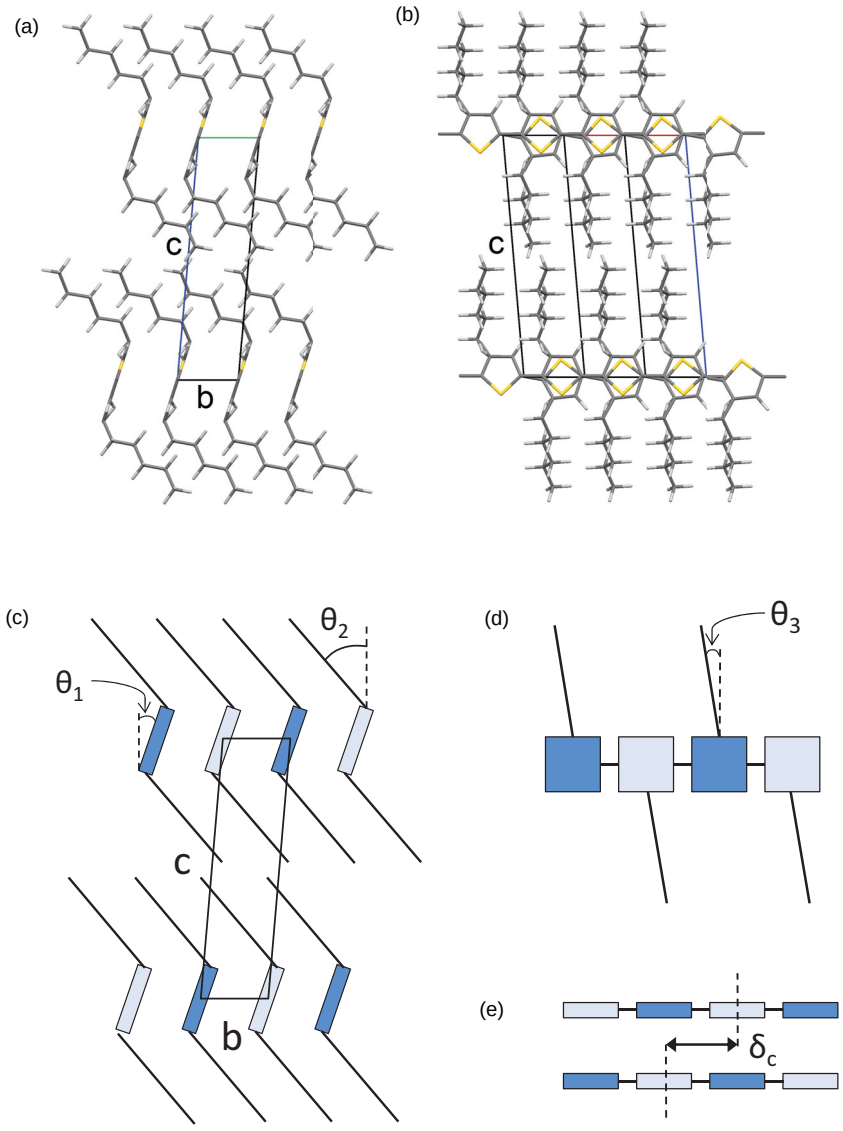

Figure 3. Best-fit molecular packing motif for $(3HT)_{13}$. The molecules exhibit a triclinic unit cell, tilted backbones and side chains, and a one thiophene shift in adjacent chains. a) Fitted structure viewed along *a*-axis. b) Fitted structure viewed parallel to *ab*-plane. c) Schematic structure viewed along *a*-axis. d) Schematic structure viewed perpendicular to plane containing thiophene backbones. e) Schematic structure viewed parallel to plane containing thiophene backbone.

molecular weight P3HT (≈7.9 kDa) which had been epitaxially crystallized from 1,3,5-trichlorobenzene (TCB). The structure described herein is quite similar to their proposed structure with a comparable tilt in the thiophene backbone as well as a relatively large tilt in the alkyl side chains, although our fitted structure suggests an even larger tilt than that found by Kayunkid.[25] We also find that the alkyl side chains come off the $(3HT)_{13}$ oligomer nearly perpendicular to the thiophene backbone, in significant agreement to the structure proposed by Kayunkid.[25] Despite the many similarities between the two models, one key difference is found in the relative shift in the thiophene backbones on adjacent chains, δ_c. The Kayunkid model finds this shift to be a fraction of a thiophene unit while we find this shift to be exactly one thiophene ring. This one-ring shift between the adjacent chains reduces the steric hindrance associated with the alkyl side chains and demonstrates that the packing of $(3HT)_{13}$ results in considerable electronic overlap between thiophene rings on neighboring molecules. One possible explanation for this discrepancy may be the difference in processing conditions of the two samples as Kayunkid's model is based on a slowly crystallized sample on a TCB substrate while our samples are wire-bar coated on silicon with a native oxide layer.

In contrast, we compare our structure to one of the most detailed structural studies conducted by DFT, that of Maillard and Rochefort.[26] Their model also contains a slight tilt to the thiophene backbone as well as a shift of exactly one thiophene unit in adjacent polymer chains, in agreement with the work presented here. The structure by Maillard and Rochefort[26] however predicts significant differences in the tilting of the alkyl side chains with respect to the chain backbone as demonstrated in Table 1. DFT calculations predict a structure that is energy minimized in vacuo and therefore neither account for the solvent that is used during the wire-bar coating nor do they take into account the polymer–substrate interactions which are known to affect P3HT structure significantly.[41] We note that while a 13-mer oligomer of P3HT was used in the present structural refinement for its high degree of crystallinity, we are confident these results are pertinent to higher weight materials. Koch et al. demonstrated that the π-stacking distance differs by less than 2% between $(3HT)_{13}$ and P3HT with a molar mass of over 200 kDa.[35] The same peaks are visible for both fractions in GIXD images, with disorder-induced broadening appearing as the most significant difference between the two. Thus, we believe that while high and low molecular weight polymers likely exhibit very minor differences in their unit cells, the vast majority of the structural and electronic insights uncovered at low molecular weights will also be applicable to higher molecular weight materials.

Table 1. Optimized structural orientation parameters for P3HT using various experimental techniques.[25,26] Diagrams of the angles and their relationship to the P3HT structure can be found in Figure 3c,d.

Method	θ_1 [deg]	θ_2 [deg]	θ_3 [deg]
This work (XRD)	19	51	8
Kayunkid (SAED)	26	29	0
Maillard (DFT)	7	−39	34

2.2. Molecular Packing in P3EHT

To determine the molecular packing in P3EHT, our first task in the refinement process is to determine the unit cell of P3EHT. In order to produce a well-defined diffraction pattern with minimal overlap between peaks, we performed an annealing treatment to the spin-cast P3EHT thin film (M_w = 6.9 kDa, M_n = 6.5 kDa) wherein the film is first melted at 120 °C and allowed to slowly recrystallize at ≈50–55 °C over 24 h. As shown in Figure 2c, the fabricated film is nearly 100% edge-on and exhibits a large number of diffraction peaks in comparison to patterns previously reported by Boudouris et al.[42] Within this latter publication, the authors also proposed the following triclinic unit cell for P3EHT: a = 7.3 Å, b = 10.3 Å, c = 15.4 Å, α = 72°, β = 98°, and γ constrained to 90°. Our efforts at structural refinements using this unit cell, however, proved to be unsuccessful and we believe for several reasons that the proposed parameters are not correct. First, no distinct crystallographic vector exists within the a–b plane whose length is a multiple of the thiophene dimer. This requirement is intrinsic to polymeric systems and arises from the fact that, with respect to the unit cell, the polymer chain is infinitely long and must represent a crystallographic direction. Any misalignment between the long chain axis and the corresponding principal unit cell axis (here axis a) would be unphysical and violate the assumption made a priori that a unit cell exists. Therefore, in determining the alignment of P3EHT in the unit cell, we place the chain backbone along the a-axis and fix the axis length at the widely reported value of 7.72 Å for a thiophene dimer. Second, although more symmetry exists in P3HT crystals and γ can be set to 45° or 90°, the same is not true in the case of P3EHT. We instead performed parameter optimization based on observed diffraction peak positions, which yields the following triclinic unit cell: a = 7.72 Å, b = 10.83 Å, c = 15.16 Å, α = 69.84°, β = 103.03°, and γ = 109.86°. With respect to the optimized $(3HT)_{13}$, the unit cell for P3EHT is more than twice the volume of the former (1110 vs 462 Å^3) and exhibits a slightly lower mass density of 1.16 g mL^{-1}. These initial observations suggest that there are two inequivalent chains, represented by two thiophene dimers within the unit cell, and that the polymer chains are not as closely packed as those of $(3HT)_{13}$.

Due to the fact that there are two dimers within the basic unit cell and that each dimer contains a large number of side chain carbons, it is not rigorously possible to determine the side chain conformations simply because of the corresponding large number of degrees of freedom that is contrasted by an only moderate number of available diffraction peaks. In addition, the extra ethyl group introduces many more degrees of freedom to the side chains such that introducing molecular hinges as previously described can also not capture the alkyl chains' molecular conformations. To simplify the problem, we first opted to remove the side chains and use instead a single carbon attached directly to the thiophene backbone; i.e., there are only two side chain carbons per dimer. This substitution is appropriate for two reasons. First, the side chains in P3EHT are thought to be highly disordered and quite mobile at room temperature, suggesting they contribute little to the observed diffraction peaks. Second, as scattered X-ray intensity increases in an approximately quadratic fashion with atomic mass, the chain backbone and the heavy sulfur atoms it contains will constitute the large majority of the observed diffraction signal. In addition, because we force the chain backbone to lie along the a-axis, we are able to reduce the number of parameters per unit cell to only three: the rotation angle for each dimer around the a-axis (2) and the sliding distance of one dimer along the same axis (1). The optimized structure and the corresponding diffraction peak intensities are plotted in Figure 2c,d.

Although the fit does not perfectly match experiment results due to the lack of side-chain carbons and details regarding their exact molecular conformations, we are able to reproduce many of the relative intensity differences between diffraction peaks. Among the (01L) set of peaks at $q_{xy} \approx 0.6$ Å^{-1}, for instance, our simulated data correctly predict that the (012) intensity is lower than those of (013), (014), and (015). In addition, the (121) and (122) peaks are shown to be the highest diffracting peaks among the (12L) Bragg rod at $q_{xy} \approx 1.2$ Å^{-1} while the cluster of peaks between 1.5 and 2.0 Å^{-1} in q_{xy} are among the weakest diffracting peaks. Both of these results agree well with the experimental data.

The simulated crystal structure is shown in **Figure 4** and exhibits several interesting properties. First, we note that adjacent polymer chain backbones are not symmetrically equivalent. The θ_1 angles for the two dimers are 21° and 49.1° for each set of adjacent chains, respectively. Note that the θ_1 value for the first chain is similar to the simulated 19° angle for $(3HT)_{13}$. The difference in angle between two adjacent chains for P3EHT is ≈28° and the chains are shifted by ≈5.53 Å. In addition, the proposed structure shows that P3EHT exhibits tighter alkyl stacking (≈14.1 Å) and much larger π-stacking distance (≈5.09 Å) as compared to the $(3HT)_{13}$ case. The large difference in π–π spacing observed between P3EHT and P3HT is especially surprising, considering previous studies concluded they were likely very similar to each other.[42] These findings are in agreement with the higher rotation angle (θ_1), lower mass density of the simulated structure, and lower hole mobility in P3EHT.[43] The larger π-stacking distance also explains the fact that the absorption onset for aggregated P3EHT is ≈100 meV blue-shifted from that of P3HT.[42] Finally, we also point out here that the sliding distance between adjacent chains is not a multiple of the thiophene monomer length as in the case of $(3HT)_{13}$, which may be a result of the asymmetric alkyl side

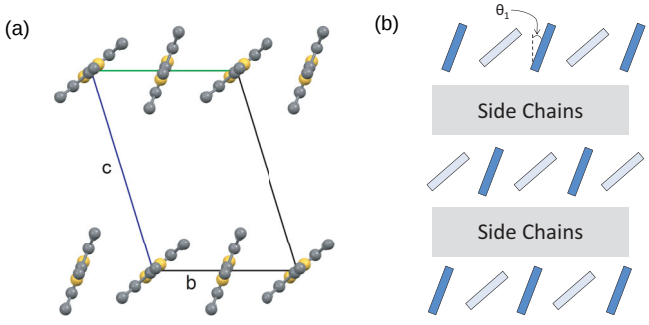

Figure 4. Best-fit molecular packing motif for P3EHT. The molecules exhibit a triclinic unit cell with a tilt difference of 28° between adjacent chain backbones. a) Fitted structure viewed along a-axis. b) Schematic structure viewed along a-axis.

Table 2. Summarized structural properties of $(3HT)_{13}$ and P3EHT. The asterisk indicates the mobility value is for a higher molecular weight version of P3HT than studied in the present work.

Unit cell parameters	$(3HT)_{13}$	P3EHT
a	7.72 Å	7.72 Å
b	5.46 Å	10.83 Å
c	15.60 Å	15.16 Å
α	96.91°	69.84°
β	94.88°	103.03°
γ	45.00°	109.86°
Unit cell volume	462 Å^3	1110 Å^3
Density	1.19 g mL^{-1}	1.16 g mL^{-1}
Alkyl-stacking distance	16.2 Å	14.1 Å
π-stacking distance	3.86 Å	5.09 Å
Hole mobility on SiO_2	$\approx 10^{-3}$ cm^2 V^{-1} s^{-1}*	$\approx 10^{-5}$ cm^2 V^{-1} s^{-1}

chains. **Table 2** summarizes the various structural differences between $(3HT)_{13}$ and P3EHT.

2.3. Electronic Structure Calculations

Calculations were preformed to determine how the structural differences brought about by the different side chains affect the electronic structure of P3HT and P3EHT. The calculations were performed for infinite periodic structures having the experimentally determined lattice vectors and molecular orientations. The alkyl chains were substituted by methyl groups in both cases. This replacement is not expected to have an effect on the dispersion of the states. The dispersion relations for two hole bands (*h*1 and *h*2) and two electron bands (*e*1 and *e*2) are shown in **Figure 5** and were obtained within DFT employing methods described in ref. [44].

The dispersion of the topmost valence band (labeled *h*1) along the direction parallel to the conjugated backbone (the *x*-direction in Figure 5) is similar in the two materials. The dispersion is 2.0 eV for P3HT and 1.6 eV for P3EHT, indicating that charge transport along the chain backbone is likely comparable in the two materials. This similarity arises because the atomic structure within the conjugated backbones is not affected strongly by the side chains. However, there is a significant difference in the dispersion of *h*1 along the π-stacking direction, the *y*-direction in Figure 5. The energy width of h1 along the π-direction is 0.3 eV for the P3HT structure, but only ≈0.02 eV for P3EHT. The substantial differences seen in the electronic structure of P3EHT in comparison to P3HT, namely, the significantly lower dispersion in P3EHT in the π-direction, arise from its much larger π–π spacing and from the large and inequivalent tilting of the two polymers in each cell (Figure S3, Supporting Information). This weak interchain coupling in P3EHT is in agreement with the low hole mobility observed in P3EHT in comparison to P3HT. Indeed, given that the energy bandwidth in P3EHT along the π-direction is less than k_BT, and comparable to phonon energies, it seems clear that the mobility and the temperature dependence of the mobility would differ significantly in the two materials.

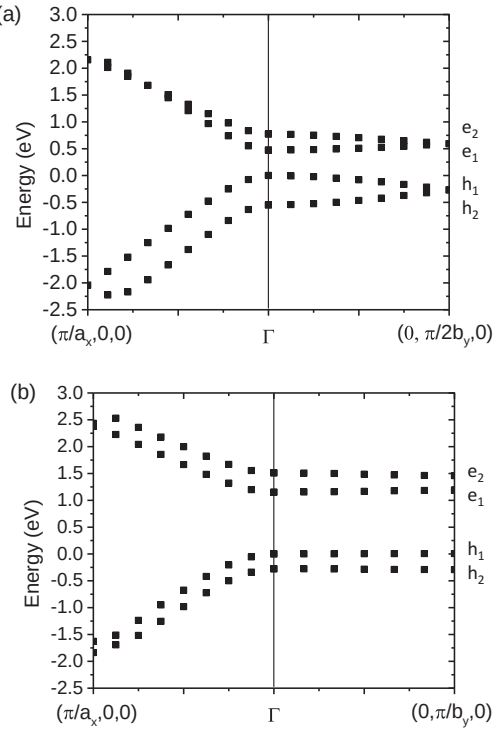

Figure 5. Band structures calculated by DFT from refined crystallographic structures for a) $(3HT)_{13}$ and b) P3EHT. The dispersion in the π-stacking direction (*y*-direction) is significantly larger for P3HT, a likely explanation for its higher charge carrier mobility.

3. Conclusion

We have presented a common methodology which can be used to calculate the precise molecular packing of a semicrystalline polymer from a simple 2D grazing incidence X-ray diffraction image. While a number of the newly introduced high-mobility donor–acceptor copolymers are very disordered and do not diffract strongly, many exhibit significant amounts of crystallization and should be amenable to the structural refinement technique described herein.[1,11,45–49] Owing to the large number of heavy atoms in the chain backbones of these materials and frequent incorporation of disordered, branched side chains, simplifications in the refinement procedure similar to those employed here for P3EHT are appropriate, and will facilitate structural determinations in these materials. This technique will enable the exact backbone packing structure of a multitude of new high-mobility polymers to be calculated for the first time and, when coupled with electronic structure calculations, will lead to significant enhancements in our understanding of these materials.

The structures presented here represent the first exact structure determination of semiconducting polymers which have been processed in the same manner with which one would produce an electronic device. This result represents a significant achievement, as processing is known to impact structure, sometimes dramatically, and yields interesting insights into the molecular structure in a technologically relevant sample. Measurements such as those presented here, which go beyond the simple unit cell determination to study exact molecular

packing, will prove invaluable for electronic property calculations and allow for the improvement of models which attempt to link structural properties to macroscopic electronic measurements. Further, the method described herein is quite general and can be expanded to determine the structure of any semicrystalline polymer that yields enough diffraction spots to perform the crystallographic refinement.

4. Experimental Section

Polymer Synthesis: Unless otherwise noted, reagents and solvents were used as received from Sigma-Aldrich. Degassed tetrahydrofuran (THF) was purified by passage through an activated alumina column (Advanced Specialty Gas Equipment, 7 × 12 mesh) and was collected in flame-dried, air-free flasks. P3EHT was synthesized using the GRIM procedure as established in the literature[50,51] and conducted as previously described.[52] P3HT was synthesized as previously published.[36]

Film Fabrication: Samples were prepared on native oxide silicon and were sonicated in acetone and isopropyl alcohol before drying with nitrogen and undergoing UV ozone treatment (20 min). Films were cast from ≈10 mg mL^{-1} solutions from toluene, by wire-bar coating at 50 °C.

Diffraction Measurements: GIXD measurements were carried out at the Stanford Synchrotron Radiation Laboratory (SSRL) on beam line 11-3 with a photon energy of 12.73 keV. The incidence angle α of the incident beam was set to 0.1°, above the critical thickness of the semiconducting film but below that of the silicon substrate. The diffraction intensity was detected on a 2D image plate (MAR-345). The distance, *L*, between sample and detector was calibrated using a LaB_6 polycrystalline standard. The flat image plate detector records an image of the *q*-space with distorted geometry and the necessary image correction procedure, enabling direct measurement in the images, is described in more detail in a previous study.[16]

Crystallographic Refinement: Numerical integration of the diffraction peak areas and the crystallographic refinement were both performed with the software WxDiff. The Monte Carlo optimization of the crystallographic residual was performed with an in-house developed software which samples the alignment and conformation space for the polymer main chain and side chain angles within the unit cell, attempting to obtain a best fit of the integrated peak intensities to the structure factor moduli (corrected for scattering geometry, beam factors). The details of this procedure and the corresponding calculation models are described in the literature.[29] Compared to the software described elsewhere,[29] the capability to model additional degrees of freedom in form of bond rotations ("hinges") was added for this work in order to emulate the conformational flexibility of the side chains.

Supporting Information

Supporting Information is available from the Wiley Online Library or from the author.

Acknowledgements

A.S. acknowledges funding from the National Science Foundation (Grant No. DMR 1205752). This work is partly supported by the German Research Foundation (DFG) within the Cluster of Excellence "Center for Advancing Electronics Dresden." The work at PARC (J.E.N.) was supported by the AFOSR under Grant No. FA9550-13-1-0106. Use of the Stanford Synchrotron Radiation Lightsource, SLAC National Accelerator Laboratory, is supported by the U.S. Department of Energy, Office of Science, Office of Basic Energy Sciences under Contract No. DE-AC02-76SF00515.

Received: January 9, 2015
Revised: February 17, 2015
Published online: March 24, 2015

[1] I. Kang, H.-J. Yun, D. S. Chung, S.-K. Kwon, Y.-H. Kim, *J. Am. Chem. Soc.* **2013**, *135*, 14896.
[2] D. Dang, W. Chen, S. Himmelberger, Q. Tao, A. Lundin, R. Yang, W. Zhu, A. Salleo, C. Müller, E. Wang, *Adv. Energy Mater.* **2014**, *4*, 1400680.
[3] Y. Zhou, T. Kurosawa, W. Ma, Y. Guo, L. Fang, K. Vandewal, Y. Diao, C. Wang, Q. Yan, J. Reinspach, J. Mei, A. L. Appleton, G. I. Koleilat, Y. Gao, S. C. B. Mannsfeld, A. Salleo, H. Ade, D. Zhao, Z. Bao, *Adv. Mater.* **2014**, *26*, 3767.
[4] J. Mei, Z. Bao, *Chem. Mater.* **2014**, *26*, 604.
[5] A. Facchetti, M.-H. Yoon, C. L. Stern, H. E. Katz, T. J. Marks, *Angew. Chem. Int. Ed.* **2003**, *42*, 3900.
[6] A. Facchetti, M.-H. Yoon, C. L. Stern, G. R. Hutchison, M. A. Ratner, T. J. Marks, *J. Am. Chem. Soc.* **2004**, *126*, 13480.
[7] J. E. Anthony, *Chem. Rev.* **2006**, *106*, 5028.
[8] T. Lei, J.-H. Dou, J. Pei, *Adv. Mater.* **2012**, *24*, 6457.
[9] H. Bronstein, D. S. Leem, R. Hamilton, P. Woebkenberg, S. King, W. Zhang, R. S. Ashraf, M. Heeney, T. D. Anthopoulos, J. de Mello, I. McCulloch, *Macromolecules* **2011**, *44*, 6649.
[10] I. Meager, R. S. Ashraf, S. Rossbauer, H. Bronstein, J. E. Donaghey, J. Marshall, B. C. Schroeder, M. Heeney, T. D. Anthopoulos, I. McCulloch, *Macromolecules* **2013**, *46*, 5961.
[11] J. Mei, D. H. Kim, A. L. Ayzner, M. F. Toney, Z. Bao, *J. Am. Chem. Soc.* **2011**, *133*, 20130.
[12] A. T. Yiu, P. M. Beaujuge, O. P. Lee, C. H. Woo, M. F. Toney, J. M. J. Fréchet, *J. Am. Chem. Soc.* **2012**, *134*, 2180.
[13] V. Ho, B. W. Boudouris, R. A. Segalman, *Macromolecules* **2010**, *43*, 7895.
[14] J. L. Brédas, J. P. Calbert, D. A. da S. Filho, J. Cornil, *Proc. Natl. Acad. Sci. U.S.A.* **2002**, *99*, 5804.
[15] M. Brinkmann, *J. Polym. Sci., Part B: Polym. Phys.* **2011**, *49*, 1218.
[16] M. Brinkmann, P. Rannou, *Adv. Funct. Mater.* **2007**, *17*, 101.
[17] D. Dudenko, A. Kiersnowski, J. Shu, W. Pisula, D. Sebastiani, H. W. Spiess, M. R. Hansen, *Angew. Chem. Int. Ed.* **2012**, *51*, 11068.
[18] D. H. Kim, J. T. Han, Y. D. Park, Y. Jang, J. H. Cho, M. Hwang, K. Cho, *Adv. Mater.* **2006**, *18*, 719.
[19] J. Mårdalen, E. J. Samuelsen, O. R. Gautun, P. H. Carlsen, *Synth. Met.* **1992**, *48*, 363.
[20] T. J. Prosa, M. J. Winokur, J. Moulton, P. Smith, A. J. Heeger, *Macromolecules* **1992**, *25*, 4364.
[21] K. Tashiro, M. Kobayashi, T. Kawai, K. Yoshino, *Polymer* **1997**, *38*, 2867.
[22] J. Mårdalen, E. J. Samuelsen, O. R. Gautun, P. H. Carlsen, *Solid State Commun.* **1991**, *80*, 687.
[23] S. Dag, L.-W. Wang, *J. Phys. Chem. B* **2010**, *114*, 5997.
[24] C. Melis, L. Colombo, A. Mattoni, *J. Phys. Chem. C* **2011**, *115*, 576.
[25] N. Kayunkid, S. Uttiya, M. Brinkmann, *Macromolecules* **2010**, *43*, 4961.
[26] A. Maillard, A. Rochefort, *Phys. Rev. B* **2009**, *79*, 115207.
[27] J. Rivnay, S. C. B. Mannsfeld, C. E. Miller, A. Salleo, M. F. Toney, *Chem. Rev.* **2012**, *112*, 5488.
[28] M. L. Chabinyc, L. H. Jimison, J. Rivnay, A. Salleo, *MRS Bull.* **2008**, *33*, 683.
[29] D. L. Cheung, D. P. McMahon, A. Troisi, *J. Phys. Chem. B* **2009**, *113*, 9393.

[30] G. Giri, E. Verploegen, S. C. B. Mannsfeld, S. Atahan-Evrenk, D. H. Kim, S. Y. Lee, H. A. Becerril, A. Aspuru-Guzik, M. F. Toney, Z. Bao, *Nature* **2011**, *480*, 504.
[31] S. C. B. Mannsfeld, M. L. Tang, Z. Bao, *Adv. Mater.* **2011**, *23*, 127.
[32] S. C. B. Mannsfeld, A. Virkar, C. Reese, M. F. Toney, Z. Bao, *Adv. Mater.* **2009**, *21*, 2294.
[33] Q. Yuan, S. C. B. Mannsfeld, M. L. Tang, M. F. Toney, J. Lüning, Z. Bao, *J. Am. Chem. Soc.* **2008**, *130*, 3502.
[34] Q. Yuan, S. C. B. Mannsfeld, M. L. Tang, M. Roberts, M. F. Toney, D. M. DeLongchamp, Z. Bao, *Chem. Mater.* **2008**, *20*, 2763.
[35] F. P. V. Koch, J. Rivnay, S. Foster, C. Müller, J. M. Downing, E. Buchaca-Domingo, P. Westacott, L. Yu, M. Yuan, M. Baklar, Z. Fei, C. Luscombe, M. A. McLachlan, M. Heeney, G. Rumbles, C. Silva, A. Salleo, J. Nelson, P. Smith, N. Stingelin, *Prog. Polym. Sci.* **2013**, *38*, 1978.
[36] F. P. V. Koch, P. Smith, M. Heeney, *J. Am. Chem. Soc.* **2013**, *135*, 13695.
[37] F. P. V. Koch, M. Heeney, P. Smith, *J. Am. Chem. Soc.* **2013**, *135*, 13699.
[38] M. Brinkmann, P. Rannou, *Macromolecules* **2009**, *42*, 1125.
[39] A. T. Brünger, *Acta Crystallogr. A* **1989**, *45*, 42.
[40] R. J. Kline, D. M. DeLongchamp, D. A. Fischer, E. K. Lin, L. J. Richter, M. L. Chabinyc, M. F. Toney, M. Heeney, I. McCulloch, *Macromolecules* **2007**, *40*, 7960.
[41] L. H. Jimison, S. Himmelberger, D. T. Duong, J. Rivnay, M. F. Toney, A. Salleo, *J. Polym. Sci., Part B: Polym. Phys.* **2013**, *51*, 611.
[42] B. W. Boudouris, V. Ho, L. H. Jimison, M. F. Toney, A. Salleo, R. A. Segalman, *Macromolecules* **2011**, *44*, 6653.
[43] D. T. Duong, V. Ho, Z. Shang, S. Mollinger, S. C. B. Mannsfeld, J. Dacuña, M. F. Toney, R. Segalman, A. Salleo, *Adv. Funct. Mater.* **2014**, *24*, 4515.
[44] J. E. Northrup, *Phys. Rev. B* **2007**, *76*, 245202.
[45] B. Sun, W. Hong, Z. Yan, H. Aziz, Y. Li, *Adv. Mater.* **2014**, *26*, 2636.
[46] J. Rivnay, R. Steyrleuthner, L. H. Jimison, A. Casadei, Z. Chen, M. F. Toney, A. Facchetti, D. Neher, A. Salleo, *Macromolecules* **2011**, *44*, 5246.
[47] H. G. Kim, B. Kang, H. Ko, J. Lee, J. Shin, K. Cho, *Chem. Mater.* **2015**, *27*, 829.
[48] G. Kim, S.-J. Kang, G. K. Dutta, Y.-K. Han, T. J. Shin, Y.-Y. Noh, C. Yang, *J. Am. Chem. Soc.* **2014**, *136*, 9477.
[49] J. Lee, A.-R. Han, H. Yu, T. J. Shin, C. Yang, J. H. Oh, *J. Am. Chem. Soc.* **2013**, *135*, 9540.
[50] R. S. Loewe, S. M. Khersonsky, R. D. McCullough, *Adv. Mater.* **1999**, *11*, 250.
[51] R. S. Loewe, P. C. Ewbank, J. Liu, L. Zhai, R. D. McCullough, *Macromolecules* **2001**, *34*, 4324.
[52] B. S. Beckingham, V. Ho, R. A. Segalman, *Macromolecules* **2014**, *47*, 8305.